Macrocycles

How to cite:
International Edition: doi.org/10.1002/anie.202006350
German Edition: doi.org/10.1002/ange.202006350

Synthesis, Characterization, and Computational Investigation of Bright Orange-Emitting Benzothiadiazole [10]Cycloparaphenylene

*Terri C. Lovell, Zachary R. Garrison, and Ramesh Jasti**

Abstract: *Conjugated aromatic macrocycles are attractive due to their unique photophysical and optoelectronic properties. In particular, the cyclic radially oriented π-system of cycloparaphenylenes (CPPs) gives rise to photophysical properties unlike any other small molecule or carbon nanomaterial. CPPs have tunable emission, possess large extinction coefficients, wide effective Stokes shifts, and high quantum yields. However, accessing bright CPPs with emissions beyond 500 nm remains difficult. Herein, we present a novel and bright orange-emitting CPP-based fluorophore showing a dramatic 105 nm red-shift in emission and striking 237 nm effective Stokes shift while retaining a large quantum yield of 0.59. We postulate, and experimentally and theoretically support, that the quantum yield remains large due to the lack of intramolecular charge transfer.*

Conjugated aromatic macrocycles have numerous benefits over their acyclic counterparts such as increased charge transport, maximized excimer emission, enhanced solubility and ability to complex guests in their cavity to create sensors or switches.[1–6] Cycloparaphenylenes (CPPs), or carbon nanohoops, are cyclic *para*-linked phenylenes with optoelectronic properties unlike any other small molecule or carbon nanomaterial (CNM).[7–12] Since their initial synthesis, these unique molecules have generated extensive interest for use as carbon nanomaterial building blocks,[13,14] organic electronic components,[15–17] novel solution- and solid-state fluorophores,[18–21] as well as polymers with novel electronic properties[22] or polymer additives.[23] Unlike other CNMs, such as carbon nanotubes (CNTs), CPPs are synthesized bottom-up via classical organic chemistry methods. This controlled, modular synthesis allows for easy and selective scaffold functionalization unattainable with other CNMs.[24–26] Additionally, their curved architecture impedes the π–π stacking observed in their linear counterparts and enhances CPP solubility.[27,28] Finally, most CPPs are brighter than similar emitting small-molecule fluorophores, they retain their fluorescent properties in aqueous media, have minimal cytotoxicity and are cell permeable making them attractive as novel biological fluorophores.[7,18,29,30]

However, bright CPPs with emissions beyond 500 nm have yet to be realized. CPP fluorescence red-shifts as the size of the nanohoop decreases, however, decreasing size leads to a dramatic decrease in quantum yield due to strain and orbital-symmetry rules.[31] For example, [10]CPP has a quantum yield of 0.46 or 0.65 (depending on the report), compared to 0.007 for [7]CPP (Figure 1).[32–34] Therefore, decreasing the size trades brightness for a red-shift in emission. Alternatively, one of the most successful approaches to influence the HOMO and LUMO energies (that is, tune the fluorescence) is incorporation of electron-donor and -acceptor units.[35–37] Simultaneously, Jasti and Itami reported different donor–acceptor CPPs with electron-acceptor units ([10]CPTcaq and aza[8]CPP, Figure 1).[38,39] However, these molecules remain afflicted with low quantum yields.

Herein, we present the first CPP where the quantum yield is not sacrificed for red-shifting the emission. BT[10]CPP (Figure 1), a [10]CPP analogue containing a single benzothiadiazole (BT) moiety, was synthesized and characterized. The inclusion of a BT unit into the CPP backbone dramatically red-shifts the [10]CPP emission profile by over 100 nm. The absorbance maximum of BT[10]CPP is virtually identical to the parent [10]CPP, resulting in a remarkable increase in the effective Stokes shift (difference between the dominant absorption and emission maxima). Remarkably, the BT[10]CPP quantum yield is essentially unaffected. We investigate this phenomenon experimentally and computationally to gain an understanding of this outcome. Through this work, we establish BT[10]CPP as the brightest orange nanohoop in this rapidly growing class of molecules.

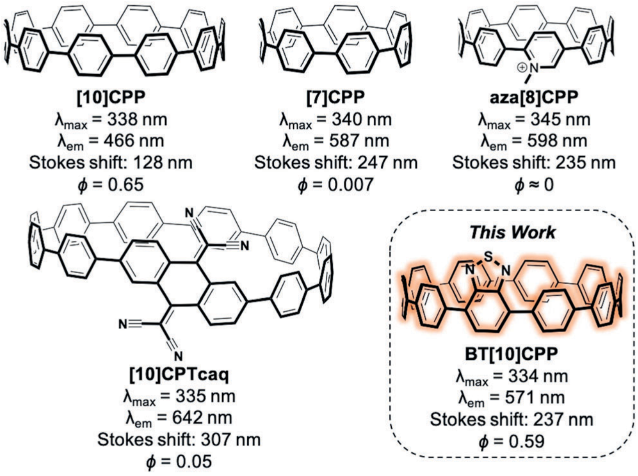

Figure 1. [10]CPP, the furthest-red-emitting nanohoops, and the novel BT[10]CPP.

---

[*] T. C. Lovell, Z. R. Garrison, Prof. Dr. R. Jasti
Department of Chemistry & Biochemistry, Materials Science Institute, and Knight Campus for Accelerating Scientific Impact, University of Oregon
Eugene, OR 97403 (USA)
E-mail: rjasti@uoregon.edu

Supporting information and the ORCID identification number(s) for the author(s) of this article can be found under: https://doi.org/10.1002/anie.202006350.

The strongly withdrawing BT moiety is well established to effectively red-shift the emission of conjugated polymers.[40–42] Thus, we set out to determine if the nanohoop emission could be tuned through BT moiety incorporation. The BT unit was incorporated into a [10]CPP scaffold via Suzuki macrocyclization of **1** and 4,7-dibromobenzo[*c*]-1,2,5-thiadiazole to yield macrocycle **2a** (Scheme 1). Triethylsilyl deprotection and mild reductive aromatization[43] afforded BT[10]CPP. A linear BT incorporated control, **3**, was synthesized for photophysical comparison through Suzuki coupling of 4,7-dibromobenzo[*c*]-1,2,5-thiadiazole and 4-methylphenylboronic acid pinacol ester. Synthesis of a smaller BT[8]CPP was also attempted. Macrocycle **4** was successfully synthesized in a similar fashion as **2a**, however, decomposition of **4** was observed. Additionally, multiple attempts to access the final BT[8]CPP through reductive aromatization were unsuccessful. We note that when H_2SnCl_4 solution was added to **4** a deep red color was observed, which quickly changed to orange. This color change may indicate formation of the desired BT[8]CPP, followed by rapid decomposition. We suspect that the instability of this molecule is the result of a high degree of strain in the smaller CPP (discussed below). BT[10]CPP and **3** were characterization by NMR (^{1}H and ^{13}C), IR, and mass spectrometry, and further analyzed by UV/Vis, fluorescence, and cyclic voltammetry.

We suspected that the instability of BT[8]CPP was the result of a high degree of strain in the smaller CPP. To quantify the strain energy in BT[10]CPP and BT[8]CPP, a strain analysis program (StrainViz) recently developed by our group was employed.[44] The total strain of each BT-containing CPP is almost identical to the analogous [*n*]CPP (Figure S13). [10]CPP has a total strain of 57.4 kcal mol^{-1} vs. 55.6 kcal mol^{-1} for BT[10]CPP. [8]CPP has a total strain of 70.5 kcal mol^{-1} vs. 70.2 kcal mol^{-1} for BT[8]CPP. Notably, there is 58 % more strain per phenylene in BT[8]CPP (8.77 kcal mol^{-1}) vs. BT[10]CPP (5.56 kcal mol^{-1}). The significant (3.2 kcal mol^{-1}) increase in strain on the BT moiety of BT[8]CPP likely causes the observed decomposition. When compared to a typical CPP phenylene unit, the BT unit should have more diene character, and thus the increased reactivity maybe another example of the effect of CPP ring size on strain-promoted reactions.[45–47]

We next characterized the photophysical properties of BT[10]CPP to determine the consequences of incorporating a BT unit into the [10]CPP scaffold. The maximum absorption of BT[10]CPP was observed at 334 nm (Figure 2a), exhibiting a minor 4 nm blue-shift compared to the parent [10]CPP.[48] A similar small blue-shift in absorption is observed in other symmetry broken nanohoops.[29,39] The extinction coefficient at the 334 nm absorbance maximum of BT[10]CPP (5.4×10^4 M^{-1} cm^{-1}) was an order of magnitude higher than that of **3** (7.6×10^3 M^{-1} cm^{-1}), but lower than [10]CPP (1.3×10^5 M^{-1} cm^{-1}).[32] The lower extinction coefficient relative to [10]CPP is unsurprising as it has been observed in the *m*[*n*]CPPs, which also possess broken symmetry. Additionally, the broken symmetry of BT[10]CPP results in a second absorption band at 445 nm (Figure 2a), which correlates to a HOMO→LUMO transition (Figure S8, Supporting Information) that is forbidden in the centrosymmetric all-hydrocarbon CPPs.[29,31] The extinction coefficient of this second transition at 445 nm was found to be 8.6×10^3 M^{-1} cm^{-1}, far lower than the absorbance maximum at 334 nm. Time-dependent density-functional theory (TD-DFT) assigned the UV/Vis absorption bands. The calculations show the HOMO→LUMO absorption band is at 445 nm. The major absorption transition at 334 nm has contributions from the HOMO→LUMO+2, HOMO−4→LUMO and HOMO−4→LUMO (Figure S8).

In contrast to the relatively minor alterations in absorbance, BT unit insertion markedly affected the emission properties. BT[10]CPP emission maximum resides at 571 nm (Figure 2a), representing a remarkable 105 nm red-

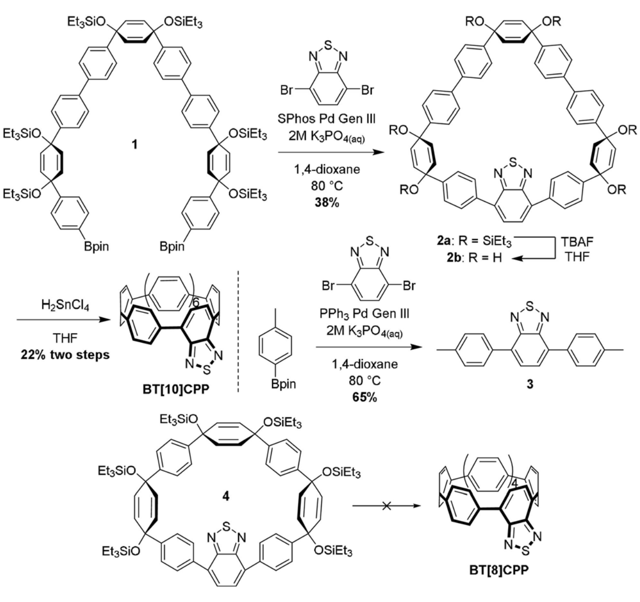

Scheme 1. Synthesis of BT[10]CPP, linear BT system **3**, and attempted synthesis of BT[8]CPP.

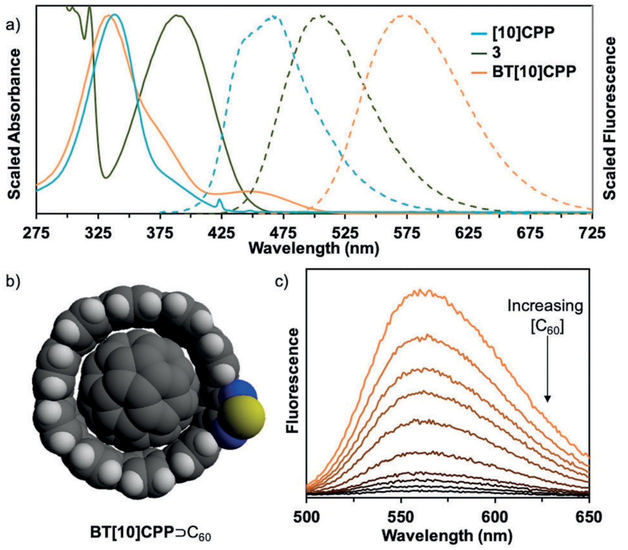

Figure 2. a) Experimental absorbance (solid line) and emission (dashed line) of BT[10]CPP and comparison to [10]CPP and **3** in dichloromethane. b) BT[10]CPP⊃C_{60} space-filling model and c) BT[10]CPP fluorescence quenching by C_{60}.

shift in emission vs. [10]CPP (466 nm).[48] As a result of this red-shifted emission, BT[10]CPP exhibits a greatly increased effective Stokes shift (237 nm, 12427 cm^{-1}) compared to [10]CPP (128 nm, 7953 cm^{-1}). Despite this, BT[10]CPP has a quantum yield of 0.59, within the range of reported values of [10]CPP (0.46[49] and 0.65[33]) and close to **3** (0.63). This was surprising considering other red-shifted nanohoops with electron accepting moieties have resulted in poor quantum yields. For example, [10]CPTcaq has a quantum yield of 0.05 and aza[8]CPP is almost non-emissive.[38,39] Thus, BT[10]CPP currently represents the brightest orange nanohoop fluorophore. To deconvolute the BT moiety contributions to the BT[10]CPP photophysical properties, we also compared to control compound **3**. Fluorescence spectroscopy of **3** revealed an emission maximum at 505 nm, 66 nm less than that of BT[10]CPP. This suggests the curved nanohoop backbone contributes significantly to the observed emission of BT-[10]CPP.

One interesting property of [10]CPP is its ability to host C_{60} with a high binding constant. A unique shape complementary host-guest interaction is formed where the intense fluorescence of [10]CPP is completely quenched by C_{60} binding.[50] We explored the host-guest properties of BT-[10]CPP with C_{60} by fluorescence-quenching experiments (Figure 2b,c). Although the fluorescence properties of the new [10]CPP-derivative have been drastically altered, the binding constant (k_a) for BT[10]CPP remains high at $(2.06 \pm 0.08) \times 10^6$ L^{-1} mol. This work and others suggest that a wide variety of fullerene hosts can be designed from the basic [10]CPP scaffold.[16]

To further explore the novel photophysical properties of BT[10]CPP, time-dependent density-functional theory (TD-DFT) calculations were performed (using Gaussian 09 and the CAM-B3LYP/6-31G* method with dichloromethane as the solvent) to analyze its electronic structure and absorption transition. The calculated frontier molecular orbitals of BT[10]CPP, [10]CPP, and [10]CPTcaq are shown in Figure 3. $S_{1'}$ is the lowest-lying excited state exhibited in CPPs, which shows exciton localization over seven phenylenes.[31] Both the $S_{1'}$ (−1.92 ev) and HOMO (−6.53 eV) energies of BT[10]CPP were lower than those of [10]CPP (−1.14 and −6.47 eV, respectively). The significantly smaller $S_{1'}\rightarrow S_0$ gap exhibited by BT[10]CPP determined by our calculations corroborates with the observed red-shifting in fluorescence. Interestingly, the HOMOs of both [10]CPP and BT[10]CPP are delocalized evenly around the hoop. However, the $S_{1'}$ (and LUMO) of BT[10]CPP is localized on the benzothiadiazole moiety. The resulting HOMO–LUMO orbital separation results in an allowed HOMO→LUMO transition, which is observed at 445 nm in the UV/Vis spectrum of BT[10]CPP. The frontier molecular orbitals provide insight into the difference in the quantum yields of BT[10]CPP and [10]CPTcaq.

As mentioned previously, a particularly anomalous discovery is the high quantum yield of BT[10]CPP despite a dramatically red-shifted emission. Based on experimental results and theoretical studies, we hypothesize that the high quantum yield is due to a lack of intramolecular charge transfer (ICT). Unlike [10]CPP and BT[10]CPP, the HOMO of [10]CPTcaq is localized on the phenylene backbone. The resultant HOMO and $S_{1'}$ orbital separation indicates the [10]CPTcaq is a donor–acceptor molecule whereas BT-[10]CPP and [10]CPP are not. Many donor–acceptor molecules exhibit ICT, which can decrease quantum yield.[51] Excited state TD-DFT calculations were used to analyze the fluorescence transitions of [10]CPP, BT[10]CPP, and [10]CPTcaq. The major fluorescence contribution of the $S_{1'}\rightarrow S_0$ transition for BT[10]CPP and [10]CPP is dominated by LUMO→HOMO contributions (Figures S10,S11). On the contrary, in [10]CPTcaq the major contribution is not from the LUMO→HOMO, but a mix of LUMO→HOMO, LUMO→HOMO−2 and LUMO→HOMO−1 contributions (Figure S12). This suggests that BT[10]CPP and [10]CPP fluoresce through a different mechanism than [10]CPTcaq. This is supported experimentally with fluorescence lifetime analysis. The fluorescence lifetime of BT[10]CPP shows monoexponential decay with a lifetime of 7.4 ns, similar to [10]CPP (6.6 ns),[49] indicating fluorescence through a similar mechanism. Finally, solvatochromism studies show ICT as a fluorescence emission pathway in [10]CPTcaq.[39] Charge-transfer emissions undergo strong red-shifting with an increase of solvent polarity.[52,53] In contrast, BT[10]CPP does not show solvatochromism (Figure S1), indicating no ICT. With the experimental and theoretical evidence given, it is concluded that the absence of ICT in this nanohoop retains the quantum yield.

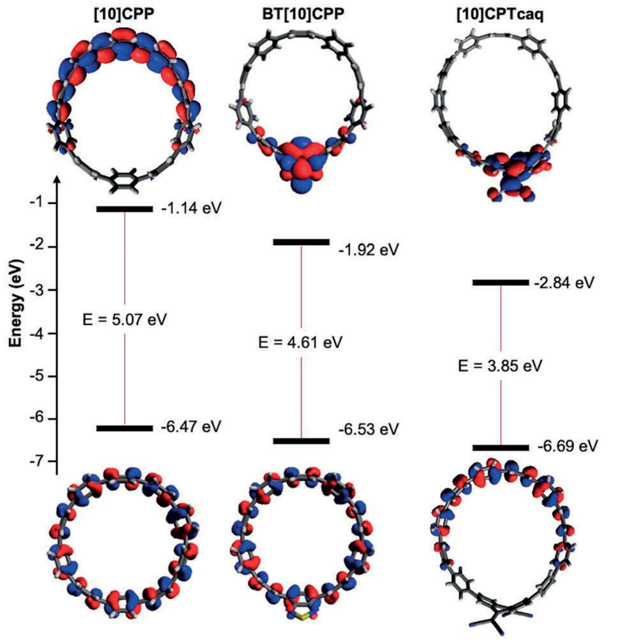

Figure 3. HOMO and $S_{1'}$ of [10]CPP, BT[10]CPP, and [10]CPTacq calculated at CAM-B3LYP/6-31G* with dichloromethane as the solvent.

In summary, we show the incorporation of a BT unit into the [10]CPP backbone allows a marked red-shifting of emission while retaining the high quantum yield of the parent CPP, resulting in the brightest orange-emitting nanohoop synthesized to date. Theoretical calculations and experimental results elucidate that BT[10]CPP does not undergo ICT, rather it is more electronically similar to the parent [10]CPP. Given that the donor–acceptor nanohoops synthesized experience both ICT and a severe drop in quantum yield, we conclude that retaining the electronic structure of the parent CPP is critical in designing bright red-emitting nanohoops. Understanding and controlling these competing photophysical pathways is important for designing bright emitting nanohoops with a variety of emission wavelength. We anticipate these nanohoops will be especially useful as biological fluorophores and further studies will be reported in due time.

Acknowledgements

Financial support was provided by the National Science Foundation (NSF) grant number CHE-1800586, and the UO OHSU Seed Grant Program. This work benefited from access to the University of Oregon high performance computer, Talapas. We would also like to gratefully acknowledge Thermo Fisher Scientific (Eugene, OR) for the use of their instrumentation.

Conflict of interest

The authors declare no conflict of interest.

Keywords: benzothiadiazoles · cycloparaphenylenes · fluorescence · macrocycles · quantum yield

---

[1] M. Ball, B. Zhang, Y. Zhong, B. Fowler, S. Xiao, F. Ng, M. Steigerwald, C. Nuckolls, *Acc. Chem. Res.* **2019**, *52*, 1068 – 1078.
[2] S. Q. Zhang, Z. Y. Liu, W. F. Fu, F. Liu, C. M. Wang, C. Q. Sheng, Y. F. Wang, K. Deng, Q. D. Zeng, L. J. Shu, et al., *ACS Nano* **2017**, *11*, 11701 – 11713.
[3] B. Zhang, M. T. Trinh, B. Fowler, M. Ball, Q. Xu, F. Ng, M. L. Steigerwald, X.-Y. Zhu, C. Nuckolls, Y. Zhong, *J. Am. Chem. Soc.* **2016**, *138*, 16426 – 16431.
[4] M. Ball, C. Nuckolls, *ACS Cent. Sci.* **2015**, *1*, 416 – 417.
[5] M. Iyoda, J. Yamakawa, M. J. Rahman, *Angew. Chem. Int. Ed.* **2011**, *50*, 10522 – 10553; *Angew. Chem.* **2011**, *123*, 10708 – 10740.
[6] H. Osaki, C.-M. Chou, M. Taki, K. Welke, D. Yokogawa, S. Irle, Y. Sato, T. Higashiyama, S. Saito, A. Fukazawa, et al., *Angew. Chem. Int. Ed.* **2016**, *55*, 7131 – 7135; *Angew. Chem.* **2016**, *128*, 7247 – 7251.
[7] E. R. Darzi, R. Jasti, *Chem. Soc. Rev.* **2015**, *44*, 6401 – 6410.
[8] S. Ghosh, R. B. Weisman, *Nat. Nanotechnol.* **2010**, *5*, 443 – 450.
[9] H. Kataura, Y. Kumazawa, Y. Maniwa, I. Umezu, S. Suzuki, Y. Ohtsuka, Y. Achiba, *Synth. Methods* **1999**, *103*, 2555 – 2558.
[10] I. Moreels, K. Lambert, D. Smeets, D. De Muynck, T. Nollet, J. C. Martins, F. Vanhaecke, A. Vantomme, C. Delerue, G. Allan, et al., *ACS Nano* **2009**, *3*, 3023 – 3030.
[11] *Optical Properties of Materials and Their Applications* (Ed.: J. Singh), Wiley, Hoboken, **2019**.
[12] G. Povie, Y. Segawa, T. Nishihara, Y. Miyauchi, K. Itami, *J. Am. Chem. Soc.* **2018**, *140*, 10054 – 10059.
[13] H. Omachi, T. Nakayama, E. Takahashi, Y. Segawa, K. Itami, *Nat. Chem.* **2013**, *5*, 572 – 576.
[14] E. J. Leonhardt, J. M. Van Raden, D. Miller, L. N. Zakharov, B. Alemán, R. Jasti, *Nano Lett.* **2018**, *18*, 7991 – 7997.
[15] E. Kayahara, L. Sun, H. Onishi, K. Suzuki, T. Fukushima, A. Sawada, H. Kaji, S. Yamago, *J. Am. Chem. Soc.* **2017**, *139*, 18480 – 18483.
[16] Y. Xu, B. Wang, R. Kaur, M. B. Minameyer, M. Bothe, T. Drewello, D. M. Guldi, M. von Delius, *Angew. Chem. Int. Ed.* **2018**, *57*, 11549 – 11553; *Angew. Chem.* **2018**, *130*, 11723 – 11727.
[17] Q. Huang, G. Zhuang, H. Jia, M. Qian, S. Cui, S. Yang, P. Du, *Angew. Chem. Int. Ed.* **2019**, *58*, 6244 – 6249; *Angew. Chem.* **2019**, *131*, 6310 – 6315.
[18] B. M. White, Y. Zhao, T. E. Kawashima, B. P. Branchaud, M. D. Pluth, R. Jasti, *ACS Cent. Sci.* **2018**, *4*, 1173 – 1178.
[19] J. M. Van Raden, B. M. White, L. N. Zakharov, R. Jasti, *Angew. Chem. Int. Ed.* **2019**, *58*, 7341 – 7345; *Angew. Chem.* **2019**, *131*, 7419 – 7423.
[20] N. Ozaki, H. Sakamoto, T. Nishihara, T. Fujimori, Y. Hijikata, R. Kimura, S. Irle, K. Itami, *Angew. Chem. Int. Ed.* **2017**, *56*, 11196 – 11202; *Angew. Chem.* **2017**, *129*, 11348 – 11354.
[21] H. Tang, Z. Gu, C. Li, Z. Li, W. Wu, X. Jiang, *Biomater. Sci.* **2019**, *7*, 2552 – 2558.
[22] G. M. Peters, G. Grover, R. L. Maust, C. E. Colwell, H. Bates, W. A. Edgell, R. Jasti, M. Kertesz, J. D. Tovar, *J. Am. Chem. Soc.* **2020**, *142*, 2293 – 2300.
[23] J. Mun, J. Kang, Y. Zheng, S. Luo, H. C. Wu, N. Matsuhisa, J. Xu, G. J. N. Wang, Y. Yun, G. Xue, et al., *Adv. Mater.* **2019**, *31*, 1903912.
[24] M. Ohfuchi, Y. Miyamoto, *Carbon* **2017**, *114*, 418 – 423.
[25] M. Moniruzzaman, K. I. Winey, *Macromolecules* **2006**, *39*, 5194 – 5205.
[26] S. Mallakpour, S. Soltanian, *RSC Adv.* **2016**, *6*, 109916 – 109935.
[27] P. Li, T. J. Sisto, E. R. Darzi, R. Jasti, *Org. Lett.* **2014**, *16*, 182 – 185.
[28] K. Meerholz, J. Heinze, *Electrochim. Acta* **1996**, *41*, 1839 – 1854.
[29] T. C. Lovell, C. E. Colwell, L. N. Zakharov, R. Jasti, *Chem. Sci.* **2019**, *10*, 3786 – 3790.
[30] L. D. Lavis, R. T. Raines, *ACS Chem. Biol.* **2008**, *3*, 142 – 155.
[31] L. Adamska, I. Nayyar, H. Chen, A. K. Swan, N. Oldani, S. Fernandez-Alberti, M. R. Golder, R. Jasti, S. K. Doorn, S. Tretiak, *Nano Lett.* **2014**, *14*, 6539 – 6546.
[32] T. Iwamoto, Y. Watanabe, Y. Sakamoto, T. Suzuki, S. Yamago, *J. Am. Chem. Soc.* **2011**, *133*, 8354 – 8361.
[33] E. R. Darzi, T. J. Sisto, R. Jasti, *J. Org. Chem.* **2012**, *77*, 6624 – 6628.
[34] T. J. Sisto, M. R. Golder, E. S. Hirst, R. Jasti, *J. Am. Chem. Soc.* **2011**, *133*, 15800 – 15802.
[35] S. Tarkuç, R. Eelkema, F. C. Grozema, *Tetrahedron* **2017**, *73*, 4994 – 5004.
[36] S. Roquet, A. Cravino, P. Leriche, O. Alévêque, P. Frère, J. Roncali, *J. Am. Chem. Soc.* **2006**, *128*, 3459 – 3466.
[37] C. Gao, L. Wang, X. Li, H. Wang, *Polym. Chem.* **2014**, *5*, 5200 – 5210.
[38] E. R. Darzi, E. S. Hirst, C. D. Weber, L. N. Zakharov, M. C. Lonergan, R. Jasti, *ACS Cent. Sci.* **2015**, *1*, 335 – 342.
[39] T. Kuwabara, J. Orii, Y. Segawa, K. Itami, *Angew. Chem. Int. Ed.* **2015**, *54*, 9646 – 9649; *Angew. Chem.* **2015**, *127*, 9782 – 9785.
[40] M. Karikomi, C. Kitamura, S. Tanaka, Y. Yamashita, *J. Am. Chem. Soc.* **1995**, *117*, 6791 – 6792.
[41] J. Hou, H. Y. Chen, S. Zhang, G. Li, Y. Yang, *J. Am. Chem. Soc.* **2008**, *130*, 16144 – 16145.
[42] M. Li, C. An, W. Pisula, K. Müllen, *Acc. Chem. Res.* **2018**, *51*, 1196 – 1205.
[43] V. K. Patel, E. Kayahara, S. Yamago, *Chem. Eur. J.* **2015**, *21*, 5742 – 5749.
[44] C. E. Colwell, T. W. Price, T. Stauch, R. Jasti, *Chem. Sci.* **2020**, *11*, 3923 – 3930.
[45] T. A. Schaub, J. T. Margraf, L. Zakharov, K. Reuter, R. Jasti, *Angew. Chem. Int. Ed.* **2018**, *57*, 16348 – 16353; *Angew. Chem.* **2018**, *130*, 16586 – 16591.
[46] P. Li, B. M. Wong, L. N. Zakharov, R. Jasti, *Org. Lett.* **2016**, *18*, 1574 – 1577.

[47] E. Kayahara, R. Qu, S. Yamago, *Angew. Chem. Int. Ed.* **2017**, *56*, 10428 – 10432; *Angew. Chem.* **2017**, *129*, 10564 – 10568.

[48] R. Jasti, J. Bhattacharjee, J. B. Neaton, C. R. Bertozzi, *J. Am. Chem. Soc.* **2008**, *130*, 17646 – 17647.

[49] M. Fujitsuka, D. W. Cho, T. Iwamoto, S. Yamago, T. Majima, *Phys. Chem. Chem. Phys.* **2012**, *14*, 14585 – 14588.

[50] T. Iwamoto, Y. Watanabe, T. Sadahiro, T. Haino, S. Yamago, *Angew. Chem. Int. Ed.* **2011**, *50*, 8342 – 8344; *Angew. Chem.* **2011**, *123*, 8492 – 8494.

[51] J. R. Lakowicz, in *Principles of Fluorescence Spectroscopy*, Springer, Baltimore, pp. 331 – 351.

[52] Z. R. Grabowski, K. Rotkiewicz, W. Rettig, *Chem. Rev.* **2003**, *103*, 3899 – 4031.

[53] C. Reichardt, *Chem. Rev.* **1994**, *94*, 2319 – 2358.

Manuscript received: May 1, 2020
Accepted manuscript online: June 8, 2020
Version of record online: ■■ ■■, ■■■■

Communications

Macrocycles

T. C. Lovell, Z. R. Garrison,
R. Jasti* ■■■■–■■■■

Synthesis, Characterization, and Computational Investigation of Bright Orange-Emitting Benzothiadiazole [10]Cycloparaphenylene

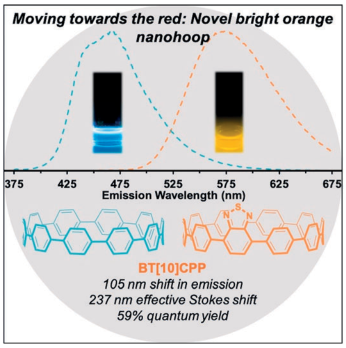

Moving towards the red: For the first time, the fluorescence of a cycloparaphenylene was dramatically red-shifted without sacrificing quantum yield. This novel cycloparaphenylene has a strong absorption, high quantum yield and shows host–guest complexation with C_{60}. Experimental and computational investigations explain its superior fluorescence properties compared to other red-shifted nanohoops.